



The flexibility of CuI chains and the functionality of pyrazine-2-thiocarboxamide keys to obtaining new Cu(I)-I coordination polymers with potential use as photocatalysts for organic dye degradation

María Murillo^a, Andrea García-Hernán^a, Jesús López^a, Josefina Perles^b, Iván Brito^c, Pilar Amo-Ochoa^{a,d,*}

^a Dpto. de Química Inorgánica, Universidad Autónoma de Madrid, 28049 Madrid, Spain

^b Laboratorio de DRX Monocristal, SIdI, Universidad Autónoma de Madrid, 28049 Madrid, Spain

^c Universidad de Antofagasta, Departamento de Química, Facultad de Ciencias Básicas, Avenida Angamos 601, Antofagasta, Chile

^d Institute for Advanced Research in Chem. Scis. (IAdChem), Universidad Autónoma de Madrid, 28049 Madrid, Spain

ARTICLE INFO

Keywords:

Coordination polymers
Crystal structures
Photo-catalysis
Photo-degradation
Water decontamination

ABSTRACT

This research focuses on two interesting aspects in the synthesis of new coordination polymers (CPs) taking advantage of the lability of coordination bonds. The first is the use of multifunctional and flexible building blocks, such as pyrazine-2-thiocarboxamide (Pyrtea) and CuI, and the second is the modification of the synthetic conditions to expand the amount of different crystalline phases. This means that starting from the same building blocks, we can increase the number of compounds obtained and diversify their final properties, as well as their possible applications. Furthermore, Cu(I)-halogen coordination polymers have been extensively studied for a long time due to their interesting optoelectronic properties. However, despite being usually semiconductors, research related to their possible behavior as photocatalysts is almost non-existent. In this work, we present five compounds, four coordination compounds with formulas $[\text{CuI}(\text{Pyrtea})]_n$ (CP1), $[\text{Cu}_3\text{I}_3(\text{Pyrtea})_7]$ (2) $[\text{Cu}_2\text{I}_2(\text{Pyrtea})]_n$ (CP4 and CP4') and a transformation of the starting ligand to a cationic imidazole derivative (compound 3) where copper iodine serves as a catalyst. All the compounds have been characterized by different techniques including single-crystal X-ray diffraction. The antibacterial behavior of CP1 against *E. Coli* DH5, *E. Coli* BL21, and *C. glabrata* (CECT 1448), as well as their optoelectronic properties, are also discussed in the work. The value of the band gap obtained (1.91 eV) for the two-dimensional coordination polymer of formula $[\text{Cu}_2\text{I}_2(\text{Pyrtea})]_n$ (CP4) allows us to study its behavior as a photocatalyst in the degradation of persistent dyes in water with interesting results, achieving a total degradation of Methylene Blue and Rhodamine B in 40 min under UV-visible light.

1. Introduction

Coordination polymers (CPs) are highly dynamic compounds obtained by self-assembly through coordination bonds of different building blocks (generally an organic ligand and a metal cation). However, these building blocks, despite their key role in the final CP structure, are not decisive. The definitive structure of the CP can vary subtly or substantially depending on the reaction conditions or synthetic methods (stoichiometry, reaction time, etc.) [1]. The final structure of the CP is crucial for its final properties and its possible applications. Therefore, a detailed study of the synthetic conditions is essential, in addition to allowing the

understanding of the chemistry of the process, it will show us the subtleties (small variations in the concentration of the reagents or the crystallization temperature, etc.) that will determine the formation of the different coordination environments, as well as the formation of different polymorphs. When we choose building blocks that show structural flexibility, the generation of different structural types responds to small variations in the synthetic conditions (which act as stimuli) and this allows us to expand and diversify the options, using the same initial ligands [2,3]. Thus, the use of CuI and organic ligands containing amino groups as building blocks gives rise to CPs with Cu(I)-I chains, highly known for their flexibility, optoelectronic properties, and

* Corresponding author at: Dpto. de Química Inorgánica, Universidad Autónoma de Madrid, 28049 Madrid, Spain.

E-mail address: pilar.amo@uam.es (P. Amo-Ochoa).

<https://doi.org/10.1016/j.cattod.2023.114072>

Received 14 December 2022; Received in revised form 24 January 2023; Accepted 26 February 2023

Available online 27 February 2023

0920-5861/© 2023 The Authors. Published by Elsevier B.V. This is an open access article under the CC BY license (<http://creativecommons.org/licenses/by/4.0/>).

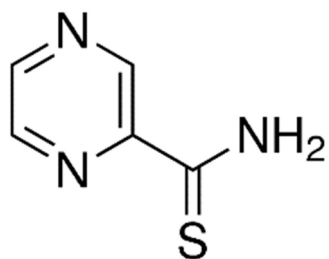


Fig. 1. Pyrazine 2-thiocarboxamide (Pyrtea).

ability to respond to stimuli by changing their structure, usually in a reversible way [4]. Additionally, CuI, with proven catalytic and electrical properties [5–7] can bind to functionalized organic ligands with various donor atoms preferable to Cu(I) such as nitrogen and/or sulfur ((Pearson's HSAB theory)). This characteristic allows us to have even more options for different CPs structures (or polymorphs) with new properties and therefore new possible applications. Thus, the use of organic ligands such as pyrazine 2-thiocarboxamide (Fig. 1), will allow expanding the structural options.

Moreover, this ligand has fungicidal and interesting redox properties [8]. Indeed, it can interact with biomolecules, such as Calf thymus DNA and Bovine serum albumin, as well as antimicrobial selectivity against *C. Albicans* [9]. Furthermore, depending on the synthetic conditions, different conformers can be stabilized. However, the literature shows us that it is not a well-studied ligand and to our knowledge, there are only a couple of Ru and Ir(III) coordination compounds studied recently from the biological point of view as possible antibacterial substances [10,11].

On the other hand, a new emerging application of CPs is photocatalysis, and some results have demonstrated that CPs are efficient photocatalysts for the degradation of organic dyes, water splitting, or photoreduction of CO₂ [12]. However, such kinds of applications of CPs on visible-light-driven photocatalysis are just beginning to emerge. How to achieve inexpensive, stable, efficient, and band-gap-tunable photocatalysts based on CPs is still a big challenge [13–15].

As we know, for photocatalytic applications we require having a relatively wide forbidden region between the HOMO and LUMO orbitals and for that fully completed *d* subshell is desired (*d*¹⁰). Therefore, Cu(I) can be used as selected metal center. On the other side, as we have already mention, a crucial requirement for these systems to be able to transition into the industry is that they must be chemically very stable (i) low cost and low toxicity (ii) systems. For the first purpose, a correct metal-ligand combination is crucial. As we have described before, the most robust coordination bonds are those established between metal-to-ligand: hard-hard or soft-soft combinations. Therefore, those based on Cu(I), a *d*¹⁰ configuration are best suited to combine with soft donor atoms (nitrogen, sulfur, or halides) containing ligands. For the second purpose, the selection of abundant metal ions, such Cu(I) as well as low cost organic ligands is crucial.

With these goals in mind, we have been able to synthesize different Cu(I)-I coordination compounds based on pyrazine 2-thiocarboxamide, some of them polymorphs, by tuning the synthetic conditions. We have also studied their properties, luminescence, electrical conductivity, antimicrobial capacity, and photo-catalytic activity versus water pollutants. In this study, methylene blue (MB) and Rhodamine B (RhB) were selected as target pollutants for degradation experiments to evaluate the catalytic performance of the CPs. Both are commonly used as representatives of widespread organic dyes that are very difficult to decompose in waste streams under light irradiation. The change in the absorption spectra of the dye solution was monitored at regular intervals of time. The decrease in absorption value of dye solution can be related in terms of the degradation efficiency.

2. Materials and methods

All reagents and solvents purchased were used without further purification. Copper Iodide (I) (CuI, 98 %) and pyrazine 2-thiocarboxamide (Pyrtea, 97 %) were purchased from Sigma Aldrich. The solvent used in the synthesis was acetonitrile (CH₃CN), purchased in Labkem and Scharlau with HPLC purification grade.

ATR-FTIR spectra were recorded with a PerkinElmer 100 spectrophotometer using a universal ATR sampling accessory from 4000 to 450 cm⁻¹. Elemental analyses were performed with a LECO CHNS-932 Elemental Analyzer. Powder X-ray diffraction data were collected using a Diffractometer PANalytical X'Pert PRO with $\theta/2\theta$ primary monochromator and X'Celerator fast detector and monochromator 1° for K α 1. The samples have been analyzed with scanning $\theta/2\theta$, from 5 to 45 degrees, with an angular increase of 0.02 and a time per increment of 100 s. Thermogravimetric analysis coupled with differential thermal analysis (TGA-DTA) was carried out on a TA Instruments Q500 thermobalance oven with a Pt sample holder. Experiments were carried out under nitrogen gas with a flow rate of 90 mL/min and a heating rate of 10 °C/min, in a range temperature from 25° to 1000°C (Figs. S14-15).

Single-crystal X-Ray diffraction (SC-XRD) measurements of compounds CP1, 2, 3A, 3B, CP4 and CP4' were conducted using a Bruker Kappa Apex II diffractometer with graphite-monochromated Mo K α radiation ($\lambda = 0.71073$ Å). The measurements were processed with the APEX4 software package. The space groups of crystals were determined using the SHELXT program, and refinements were performed using SHELXL program against F² by full-matrix least-squares refinement. Cell parameters were determined and refined by a least-squares fit of all reflections. A semi-empirical absorption correction (SADABS) was applied in all the cases. The non-hydrogen atoms were refined with anisotropic displacement parameters. All hydrogen atoms were included in their calculated positions, assigned fixed isotropic thermal parameters, and constrained to ride on their parent atoms. The crystals obtained for CP4 were extremely small and appeared as aggregates and twinned specimens and, as a consequence, *R1/wR2* values for this structure are higher than the ones obtained for the other crystalline phases. A summary of details about crystal data, collection parameters and refinement are documented in Table S1, and additional crystallographic details are provided in the CIF files.

Crystallographic data for the structures reported in this contribution have been deposited at the Cambridge Crystallographic Data Centre (CCDC) with codes CCDC 2211284 (3B), 2211285 (3A), 2211286 (CP4'), 2211288 (2), 2211289 (CP1) and 2224780 (CP4). Copies of the data can be obtained free of charge on application to the CCDC, Cambridge, U.K. (<http://www.ccdc.cam.ac.uk/>).

2.1. Electrical conductivity measurements

Two probe direct current (dc) electrical conductivity measurements at 295 K were performed in several (at least three) single crystals of compounds (Section S5.). The conductivity values were obtained by applying voltages from -10.0 to +10.0 V. The final conductivity value is given by the average value, respectively. The contacts were made with Pt wires (25 μ m diameter) using graphite paste. The samples were measured in a Quantum Design PPMS-9 equipment connected to an external voltage source (Keithley model 2400 source-meter) and amperemeter (Keithley model 6514 electro-meter).

2.2. Antibacterial assays of CP1

The Agar diffusion method was used to determine the antimicrobial activity of the CP1 using as control caspofungin, ampicillin, and voriconazole (5 μ g). Different concentrations of CP1 and Pyrtea were deposited on the agar surface of a plate-Petri previously inoculated with different microorganisms. Afterward, the dishes are incubated for 24 h at 37 °C, and thereafter, the growth of bacteria is determined.

Antimicrobial activity is indicated by the absence of bacterial growth (increasing zone diameter or halo, in mm) (Table S3). The results were negative, (0 mm halo) probably due to the insolubility of **CP1** in water.

2.3. Photo-catalytic studies

Light irradiation was performed with a 15 W purple LED photo-reactor thermostated at 20 °C. A Stellarnet model Blue-Wave UV-NB50 spectroradiometer was used to measure the emission of the purple LED used (range $\lambda = 300\text{--}600$ nm, integration time CR2-AP + 200 ms, and intensity 20.5674 W/m^2). The stoppered vials with magnetic stirring that are introduced into the reactor contain 2 mg of the $\text{C}_5\text{H}_5\text{Cu}_2\text{I}_2\text{N}_3\text{S}$ (**CP4**) and 2 mL of aqueous solution (10^{-5} M) of the Methylene blue (MB) and Rhodamine B (RhB) organic dyes respectively (Fig. 7, and S24–32). To draw the calibration line for the organic dyes and to evaluate the degradation of each dye in the samples, the UltraViolet-Visible Agilent 8453 equipment was used. For this, a stock solution of 10^{-3} M of the respective dye was prepared in water from the that were obtained by dilution 1:10 the rest of the patterns (Figs. S23 and S24).

2.4. Scanning electron microscopy (SEM) studies

The SEM images were taken on a FEI Verios 460 SEM using 2 Kv as the accelerating voltage. For the sample preparation conductive carbon tape is adhered to a SEM sample holder and the sample is glued without further treatment (Fig. S33).

2.5. Synthetic procedures

2.5.1. Room temperature synthesis of $[\text{CuI}(\text{Pyrtca})]_n$ (**CP1**), $[\text{Cu}_3\text{I}_3(\text{Pyrtca})_7]$ (**2**) and $[(\text{C}_{10}\text{H}_9\text{N}_6)(\text{HSO}_4)]$ (**3A**)

These compounds were obtained by the reactions with both stoichiometry (1:1 and 1:2 (Cu:L)) between CuI (38 mg, 0.2 mmol) and pyrazine-2-thiocarboxamide (28 mg, 0.2 mmol, and 56 mg, 0.4 mmol) respectively. Each dissolved in 4 or 6 mL of acetonitrile at 25 °C and under magnetic stirring (1600 r.p.m.) for 60 min. Immediately a black-brown precipitate (**CP1**) is formed which is centrifuged, washed with acetonitrile (2×5 mL), and air-dried. The reaction with stoichiometry 1:1 (Cu:L) generates a yield of **CP1** of 55 %, while in the reaction with stoichiometry 1:2 (Cu:L) 60 % of **CP1** is obtained, Cu-based. The mother liquors are separated into two vials respectively. One is placed in the freezer and the other is left at room temperature. In the vial left at room temperature, opaque reddish-black single crystals of **CP1** suitable for resolution by single-crystal X-ray diffraction appear after 24 h. In the reaction with stoichiometry 1:2, in the vial at room temperature after 72 h, suitable for SC-XRD crystalline orange fibers of compound **3A**, grow. Crystals are manually isolated under microscope (Yield: 40 % Cu-based).

In the vial at the freezer, a few red plate crystals of **2** suitable for resolution by single-crystal X-ray diffraction appear after 24 h (Fig. S1b). The amount of crystals obtained from this compound is so small that only allowed the characterization of this solid by single crystal X-ray diffraction.

The fit between the experimental and calculated powder X-ray diffraction (PXRD) data confirmed the structural phase purity of **CP1** and compound **3A** (Figs. S9, and S10).

2.5.2. Solvothermal synthesis of $[\text{CuI}(\text{Pyrtca})]_n$ (**CP1**), and $[(\text{C}_{10}\text{H}_9\text{N}_6)(\text{HSO}_4)]$ (**3A**) in different proportions

a) To a solution of CuI (19 mg, 0.1 mmol) dissolved in 3 mL acetonitrile, a solution of pyrazine-2-thiocarboxamide in 4 mL acetonitrile (14 mg, 0.1 mmol) was added dropwise. The mixture was sealed in a 10 mL Teflon-lined autoclave heated using solvothermal microwave-assisted activation, over 24 h at 120 °C and with slow cooling to 30 °C at a rate of 4.5 °C/h (20 h). Single crystals of **CP1** (Yield: 90 %

Cu-based) and **3A** (Yield: 10 % Cu-based) are obtained. The separation of the mixture of crystals is done manually under a microscope.

b) To a solution of CuI (19 mg, 0.1 mmol) dissolved in 3 mL acetonitrile a solution of pyrazine-2-thiocarboxamide in 4 mL acetonitrile (27.8 mg, 0.2 mmol) was added dropwise. The mixture was sealed in a 10 mL Teflon-lined autoclave heated using solvothermal microwave-assisted activation, over 24 h at 120 °C and with slow cooling to 30 °C at a rate of 4.5 °C/h (20 h). Single crystals of **CP1** (Yield: 20 % Cu-based), and **3A** (Yield: 80 % Cu-based) were obtained. The separation of the mixture of crystals is done manually under a microscope.

Elemental analysis calcd. (%) for $\text{C}_5\text{H}_5\text{CuIn}_3\text{S}$ (**CP1**): C 18.22, H 1.53, N 12.75, S 9.73; found: C 18.58, H 1.80, N 12.81, S 9.45; IR selected data (ATR) (cm^{-1}) = 3294(m), 3245(m), 3128(s), 3050(w), 1616(s), 1464(m), 1418(w), 1390(s), 1317(w), 1283(w), 1176(s), 1142(s), 1132(s), 1088(m), 1064(m), 1027(s), 972(s), 900(s), 852(s), 803(w) 754(w), 718(w), 632(w), 584(s).

Thermogravimetric analysis (TGA) was carried out for **CP1** in powder, and the results show stability until 200 °C (Fig. S13).

Elemental analysis calcd. (%) for $\text{C}_{10}\text{H}_{10}\text{N}_6\text{O}_4\text{S}$ (**3A**): C 38.71, H 3.25, N 27.09, S 10.33; found C 37.59, H 3.62, N 25.45, S 10.46. IR selected data (ATR) (cm^{-1}) = 3365(m), 3236(m), 2245(w), 1601(s), 1571(s), 1442(s), 1303(m) 1185(s), 1050(s), 1016(s), 897(m), 858(m), 758(w), 689(m), 629(m).

2.5.3. Room temperature synthesis of $[\text{Cu}_2\text{I}_2(\text{Pyrtca})]_n$ (**CP4**) and $[\text{Cu}_2\text{I}_2(\text{Pyrtca})]_n$ (**CP4'**)

The reaction is with stoichiometry 2:1 (Cu:L). A solution of pyrazine-2-thiocarboxamide (28 mg, 0.2 mmol) in 4 mL acetonitrile is added dropwise over a solution of CuI (76 mg, 0.4 mmol) in 6 mL acetonitrile at 25 °C and stirred for 1 h at 1600 rpm. In that conditions, a reddish precipitate appears immediately (**CP4**). The precipitate is separated by centrifugation, washed with acetonitrile (2×5 mL) and air dried. (Yield: 45 mg; 43 % Cu-based). Red crystals corresponding to **CP4** grow from the mother liquor at room temperature after 24 h. The crystals are separated by filtration, washed with acetonitrile and air dried. The yield obtained is 15 % Cu-Based.

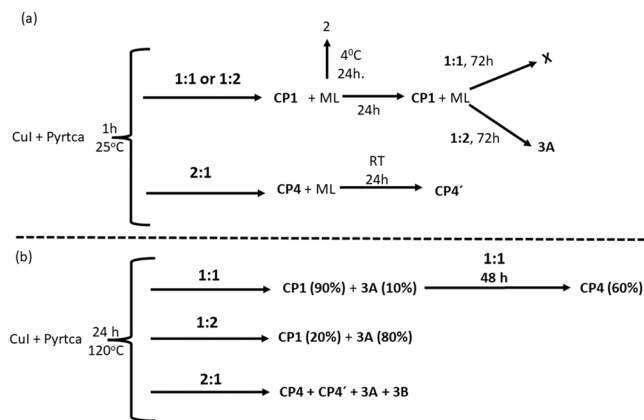
The PXRD pattern showed that the structure of the powder compound (**CP4**) does not coincide with the single crystals obtained after 24 h. at room temperature (**CP4'**). The structural phase purity of the crystals of **CP4'** was confirmed by PXRD.

To obtain good crystals of **CP4** in order to solve its structure by SC-XRD, it was necessary to carry out a solvothermal reaction. A stoichiometric reaction between CuI (19 mg, 0.1 mmol) dissolved in acetonitrile (3 mL) by adding dropwise a solution of pyrazine-2-thiocarboxamide acetonitrile (14 mg, 0.1 mmol in 4 mL) was prepared. The solution was sealed in a 10 mL Teflon-lined autoclave heated using solvothermal microwave-assisted activation, over 48 h at 120 °C. and slow cooling to 30 °C at a rate of 3.75 °C/h (24 h). Finally, an orange suspension was obtained with orange crystals (**CP4**). At that point, the orange crystals were isolated from the resulting suspension by centrifugation, and dried on air.

The phase structure purity of the single crystals of the **CP4'** was then confirmed by PXRD (Fig. S12).

Powder XRD of **CP4** matches with theoretical one from the single crystals obtained by the solvothermal method. (Fig. S11) On the other hand, recrystallization of polycrystalline **CP4** powder in acetonitrile gave rise to crystals of **CP1** after 24 h.

Elemental analysis calcd. (%) for $\text{C}_5\text{H}_5\text{Cu}_2\text{I}_2\text{N}_3\text{S}$ (**CP4** and **CP4'**): C 11.55, H 0.97, N 8.08, S 6.17; found powder: C 11.80, H 1.02, N 8.09, S 6.20 and found single crystals (**CP4'**): C 11.79 H 1.18 N 8.11 S: 6.50; IR selected data of the polycrystals (**CP4**) (ATR): (cm^{-1}) = 3355(m), 3246(m), 3138(w), 3066(w), 1591(s), 1574(s), 1444(s), 1392(w), 1310(w), 1180(m), 1164(w), 1055(s) 1019(s), 902(m), 859(s), 746(w), 591(s). IR



Scheme 1. Synthesis of CP1, 2, 3A, 3B, CP4 and CP4' in CH₃CN. Room temperature (RT/ 25°C) (a). Solvothermal conditions (b). Pyrtca= Pyrazine 2-thiocarboxamide; mL =mother liquor, X = nothing crystallizes.

selected data of the **single crystals** (ATR): (cm⁻¹) = 3355(m) 3246(m) 3138(w) 3066(w) 1591(s) 1574(s) 1444(s) 1392(w) 1310(w) 1180(m) 1164(w) 1055(s) 1019(s) 902(m) 859(s) 746(w) 591(s).

Thermogravimetric analysis (TGA) was carried out for **CP4** in powder, and the results show stability until 200 °C (Fig. S14).

2.5.4. Solvothermal synthesis of [Cu₂I₂(Pyrtca)]_n (CP4), [Cu₂I₂(Pyrtca)]_n (CP4'), [(C₁₀H₉N₆)(HSO₄)] (3A) and [(C₁₀H₉N₆)(I)] (3B)

To a solution of CuI (19 mg, 0.1 mmol) dissolved in 3 mL acetonitrile a solution of pyrazine-2-thiocarboxamide in 4 mL acetonitrile (7 mg, 0.05 mmol) was added dropwise. The mixture was sealed in a 10 mL Teflon-lined autoclave heated using solvothermal microwave-assisted activation, over 24 h at 120 °C and with slow cooling to 30 °C at a rate of 4.5 °C/h (20 h). Powder of **CP4** (Yield: 12 mg; 12 % Cu-based) together with single crystals of **CP4'**, **3A** and **3B** are obtained. The separation of the mixture of crystals is done manually under a microscope. It should be mentioned that under these conditions, the yield of the crystals corresponding to **3B** is small.

3. Results and discussion

In this work, we have evaluated the role and importance of different factors that allow the creation of a greater number of CPs' crystal structures starting from the same building blocks. We have evaluated the importance of the flexibility of CuI chains, together with the versatility of pyrazine 2-thiocarboxamide as it has several possible donor atoms (S and N). It is noteworthy that the amide group is an interesting functional group due to the two types of hydrogen bonding sites, the -C=S group working as an electron donor and the -NH₂ moiety working as the

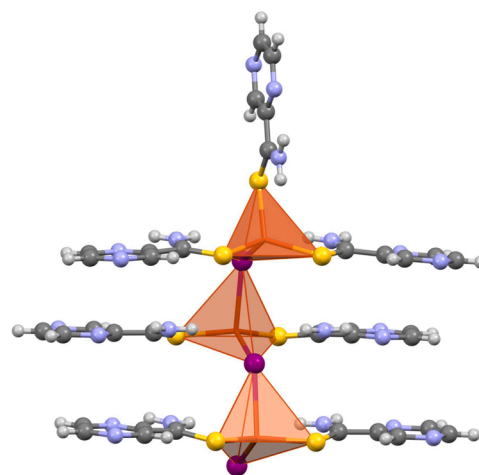


Fig. 3. Structure of trimetallic compound [Cu₃I₃(Pyrtca)₇] (2). Color code: copper (orange), iodine (purple), sulfur (yellow), carbon (grey), and nitrogen (blue).

electron acceptor. Thus, the amides induce hydrogen bonding interactions between themselves, with the counteranions, and with the solvent. Furthermore, the pyrazine can allow the extension of the structures through the two free nitrogen atoms. Furthermore, its configuration allows the metal center to be chelated through the S and Nitrogen of the pyrazine. These, together with the synthetic conditions, temperature, reaction time, and stoichiometry have made it possible to obtain five different compounds. Given the solubility of both CuI and ligand in acetonitrile, this organic solvent is chosen to carry out the reactions. Scheme 1 summarizes the conditions carried out to obtain the different compounds.

3.1. Crystal structure of [CuI(Pyrtca)]_n (CP1)

The analysis of the results obtained in the different reaction conditions shows us that in stoichiometric conditions (CuI:L1) the predominant compound is [CuI(Pyrtca)]_n (**CP1**) regardless of the temperature reaction (Scheme 1). **CP1** crystals, in the form of reddish-black prisms, suitable for the structure solution by SCXRD, can be obtained by controlled evaporation at 25°C of the mother liquor (Fig. 2 and S1a and Table S1).

CP1 is a monodimensional coordination polymer (Fig. 2) with a formula [CuI(Pyrtca)]_n. It displays a zigzag shape along the [101] direction, where the copper (I) atom displays a distorted tetrahedral CuN₂SI environment, coordinating simultaneously to one sulphur, two nitrogen atoms from two different pyrtca ligands, and a terminal iodide ligand. Regarding the Pyrtca ligand, it acts as a bridge, connecting

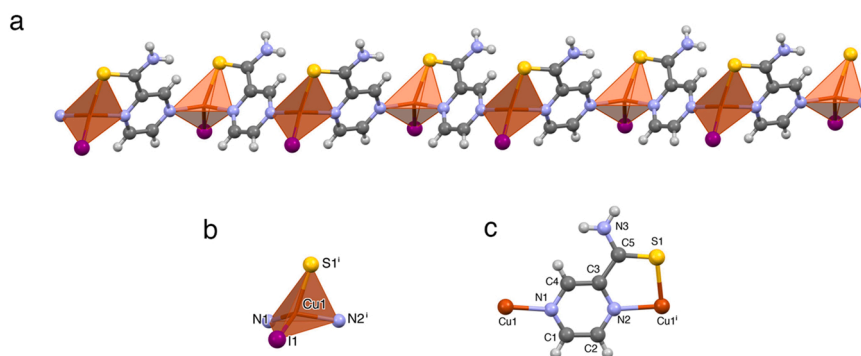
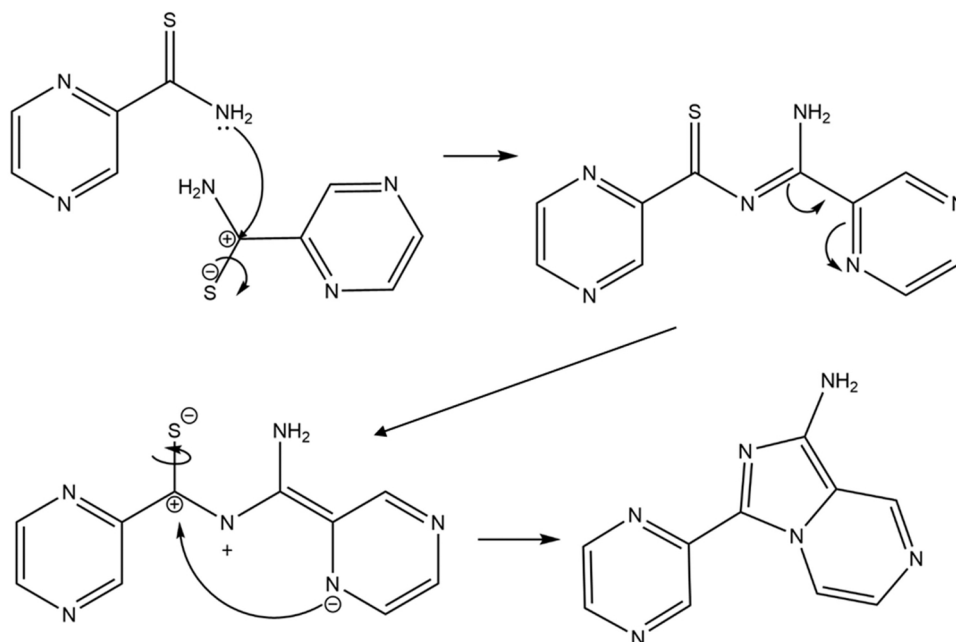


Fig. 2. Single-chain of CP1 (a), coordination environment of the copper atom (b) and coordination mode of the Pyrtca ligand (c). Copper is depicted in orange, iodine in purple, sulfur in yellow, carbon in grey, and nitrogen in blue.



Scheme 2. Proposed formation mechanism of compound 3.

two metal centres in a μ_2 - $1\kappa^2\text{N}_2\text{S}$; $2\kappa\text{N}'$ fashion. The chains in this crystal structure are closely packed by N-H...I interactions between neighbour chains.

Given the affinity of Cu(I) (electron-rich soft metal) for soft bases, it forms a 5-atom cycle as shown in Fig. 2c. We can observe that CP1 is the most stable CPs in this system due to the fact that, regardless of stoichiometry, temperature, and reaction time, it often appears (Scheme 1). Its formation is thermodynamically and kinetically favored due to the formation of the five-member chelate ring between Cu(I), S, and N atoms (Fig. 2).[16–19].

3.2. Crystal structure of $[\text{Cu}_3\text{I}_3(\text{Pyrtca})_7]$ (2)

If the mother liquor of the reaction carried out at 25°C (with both stoichiometries 1:1 and 1:2) is left for 24 h at low temperatures 4 to –20°C, small amounts of the molecular compound $[\text{Cu}_3\text{I}_3(\text{Pyrtca})_7]$ (2) can be obtained (Scheme 1a). Compound 2 is a molecular trimetallic zigzag Cu(I)-I chain where two copper(I) display a tetrahedral Cu_2I_2 environment, coordinating to two iodine and two sulfur atoms from different ligands, while the third one coordinates to one iodine and three different Pyrtca ligands in a Cu_3I tetrahedral arrangement (Fig. 3). Regarding the coordinating modes of the ligands, all of the Pyrtca ligands are terminal and coordinate only via the S atom; one of them is apical, while the other six are laterally placed; two of the iodide ligands act as bridges between two copper atoms and the third one is terminal.

The packing of the molecules in this crystal structure is achieved

mainly by π - π stacking between the pyrazine rings of neighbour molecules, with distances between centroids ranging from 3.711 to 3.784 Å.

3.3. Crystal structures of two salts of the imidazole derivative 3 as 3A, $[(\text{C}_{10}\text{H}_9\text{N}_6)(\text{HSO}_4)]$ and 3B, $(\text{C}_{10}\text{H}_9\text{N}_6)\text{I}$

Additionally, in excess of ligand, under solvothermal conditions or long reaction times, a rupture and reorganization of the ligand occurs forming a cationic imidazole derivative (compound 3), that can be obtained in crystalline phases both as the bisulfate 3A, $[(\text{C}_{10}\text{H}_9\text{N}_6)(\text{HSO}_4)]$ and as the iodide 3B, $(\text{C}_{10}\text{H}_9\text{N}_6)\text{I}$ (Scheme 1b). Crystals of compound 3A can be obtained with stoichiometry Cu/L 1:2, either with extreme conditions such as a solvothermal reaction (120°C, 24 h), where the pressure and temperature are high, or by slow evaporation and exposure to air for several days (72 h at 25°C) (Scheme 1a and b). Few crystals of compound 3B can be obtained with stoichiometry Cu/L 2:1, with solvothermal reaction (Scheme 1b). In those synthetic conditions, a reorganization of the ligands occurs, generating compound 3 favored by the presence of CuI as a possible catalyst thanks to its thiophilic property. A cyclic structure is probably obtained from the union of two ligands, releasing H_2S which reacts with oxygen from the atmosphere or water present, giving rise to 3 (Scheme 2 and Fig. 4). The formation of this type of cycle is typical of azoles [20].

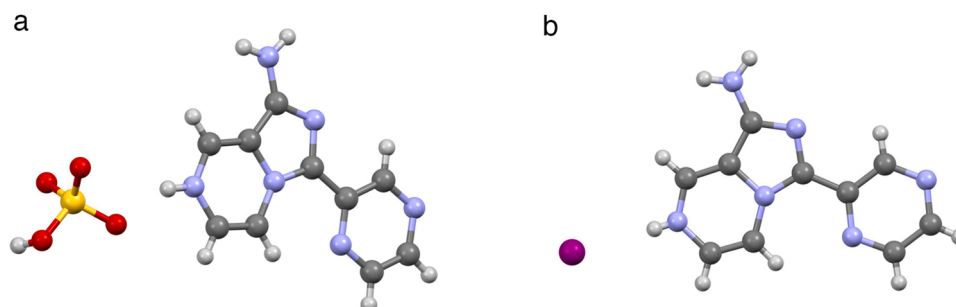


Fig. 4. Structures of 3 A (a) and 3B (b). Color code: iodine (purple), sulfur (yellow), oxygen (red), carbon (grey), and nitrogen (blue).

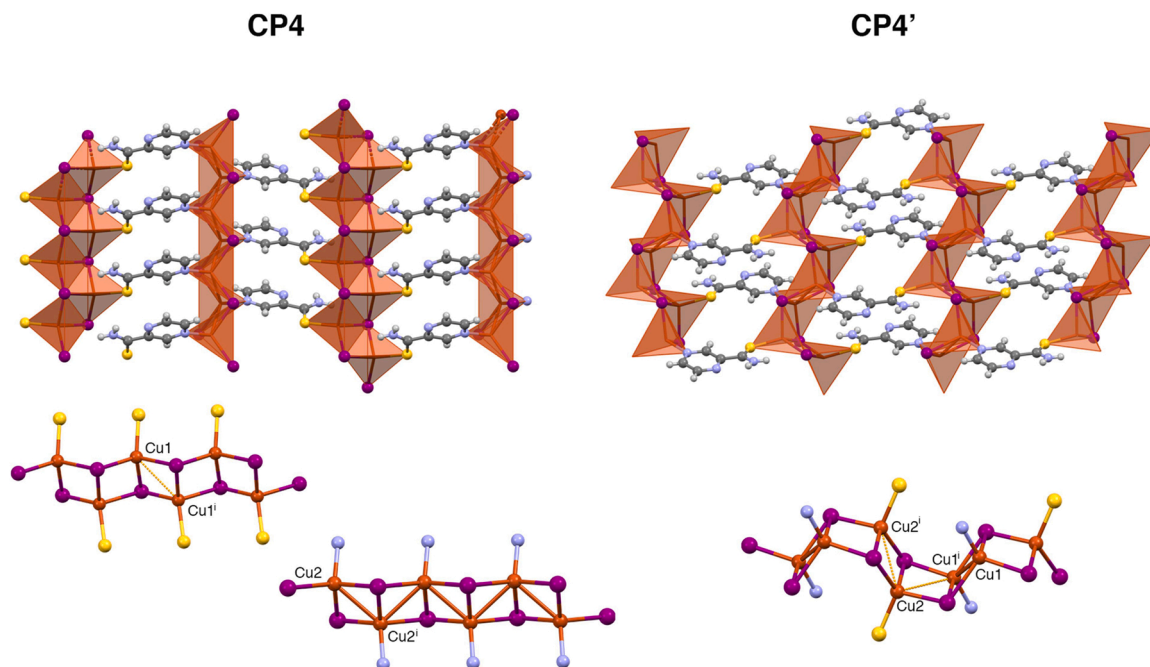


Fig. 5. Structures of CP4 (left) and CP4' (right), where the different types of Cu_2I_2 chains can be seen (bottom). In the case of CP4 (bottom left), the distance between Cu1 atoms is 3.183(8) Å, and between Cu2 atoms is 2.835(8) Å. In CP4' (bottom right), three distances can be found: $\text{Cu1}\cdots\text{Cu1}^i$ is 2.687(1) Å, $\text{Cu1}^i\cdots\text{Cu2} = 2.999(2)$ Å and $\text{Cu2}\cdots\text{Cu2}^i = 3.138(1)$ Å.

3.4. Crystal structures of $[\text{Cu}_2\text{I}_2(\text{Pyrtca})]_n$ (CP4 and CP4')

The excess of copper (I) in the reaction with stoichiometry Cu/L 2:1, allows two-dimensional coordination polymers **CP4** and **CP4'** to be obtained that display ladder-like chains with Cu_2I_2 rhombi.

Single crystals of **CP4** can be obtained at high pressures and temperatures (120 °C), and 24 h later a new polymorph (**CP4'**) from the mother liquor at room temperature or in solvothermal conditions is obtained (Scheme 1a and b). The experimental PXRD pattern of the red precipitate (**CP4**) in the reaction was compared with the theoretical one calculated from the crystal structure of the phase obtained by slow evaporation (**CP4'**) (Scheme 1 and Fig. S11). It was observed that they did not coincide. However, both the IR (Fig. S19) and elemental analysis did, indicating that it was a polymorph. To obtain the single crystals suitable for its solution using SCXRD, alternative ways were explored. Employing a solvothermal synthesis in CH_3CN with 1:1 (48 h) or 1:2 (24 h) stoichiometries, orange prisms of **CP4** were obtained and the crystal structure of this compound could be solved, finding that the theoretical XRD pattern obtained for the structure of **CP4** fit the experimental one from the red powder (Fig. S11).

Both structural types can be described as two dimensional polymers of I-I edge-sharing CuAl_3 (A= N or S) copper tetrahedral, where the Pyrtca ligand acts as a bridge between two Cu(I) atoms located at adjacent chains in a μ_2 -1κN; 2κS fashion, coordinating both through the sulfur of the carboxamide group and the nitrogen atom from the pyrazine, and the iodine atoms act in a μ_3 way connecting three copper atoms from the same chain. However, the overall arrangement in **CP4** and **CP4'** is quite different (Fig. 5).

The SC-XRD structure of **CP4** reveals a two-dimensional coordination polymer in zigzag layers parallel to the (101) plane, where the Cu_2I_2 chains are parallel to the *b* axis (Fig. 5, top). Two alternating types of Cu_2I_2 chains are present (see Fig. 5, bottom left). In the one containing Cu1, the coordination environment is a CuSI_3 distorted tetrahedron where the metal atoms are located at 3.183(8) Å. In the second one, copper atoms show a CuNI_3 distorted tetrahedral environment and the Cu2-Cu2 distance is shorter (2.835(8) Å).

CP4' is also a bidimensional coordination polymer, with flat layers

parallel to the (101) plane. In this compound, there is only one type of Cu_2I_2 chain, where pairs of the two copper atoms in the asymmetric unit alternate (see Fig. 5, bottom right) with Cu1 presenting a CuNI_3 environment while the one for Cu2 is CuSI_3 . In the chains, three different distances can be found: the shortest one between Cu1 atoms ($\text{Cu1}\cdots\text{Cu1}^i = 2.687(1)$ Å) an intermediate one for $\text{Cu1}^i\cdots\text{Cu2} = 2.999(2)$ Å, and the longest one for Cu2 atoms of 3.138(1) Å.

3.5. Antibacterial assays of CP1

Due to the fungicidal properties of pyrazine 2 thiocboxamide [9], preliminary tests were carried out to determine the antimicrobial capacity of **CP1** using the agar diffusion method (section S7 supporting information), against *E. Coli* DH5, *E. Coli* BL21 and *C. glabrata* (CECT 1448). The results obtained (Table S3) were not relevant, mainly due to the high insolubility of **CP1** in the biological medium.

3.6. Opto electronic properties of CP1, CP4 and CP4'

In the case of **CP4** and **CP4'** CPs, the Cu...Cu distances (Fig. 5) allow thinking that these compounds could have cuprophilic interactions and therefore optoelectronic properties. However, qualitative studies of their luminescence behavior under UV lamps at 254 and 365 nm showed a null luminescence in the visible, probably because the ligand produced a quenching effect.

Although they do not show luminescence, they do exhibit electronic properties. In general, coordination polymers are not good conductors of electricity. However, those with Cu (I)-I chains have a semiconducting character [21,22]. The electrical conductivity of CPs **CP1**, **CP4**, and **CP4'** has been measured at 25°C on single crystals using the two-contact method. In this case, the conductivity values are 1.4×10^{-9} , 3.8×10^{-9} , and 2.8×10^{-8} S/cm, respectively which are in the normal range for them (Figs. S19–S20) and could indicate a semiconductor behavior. For this reason, the band gap of **CP1** and **CP4** was investigated by a UV/vis diffuse-reflectance measurement method at room temperature. The results give E_g (band-gap energy) values of 1.94 and 1.91 eV for **CP1** and **CP4** respectively (Figs. S21–22).

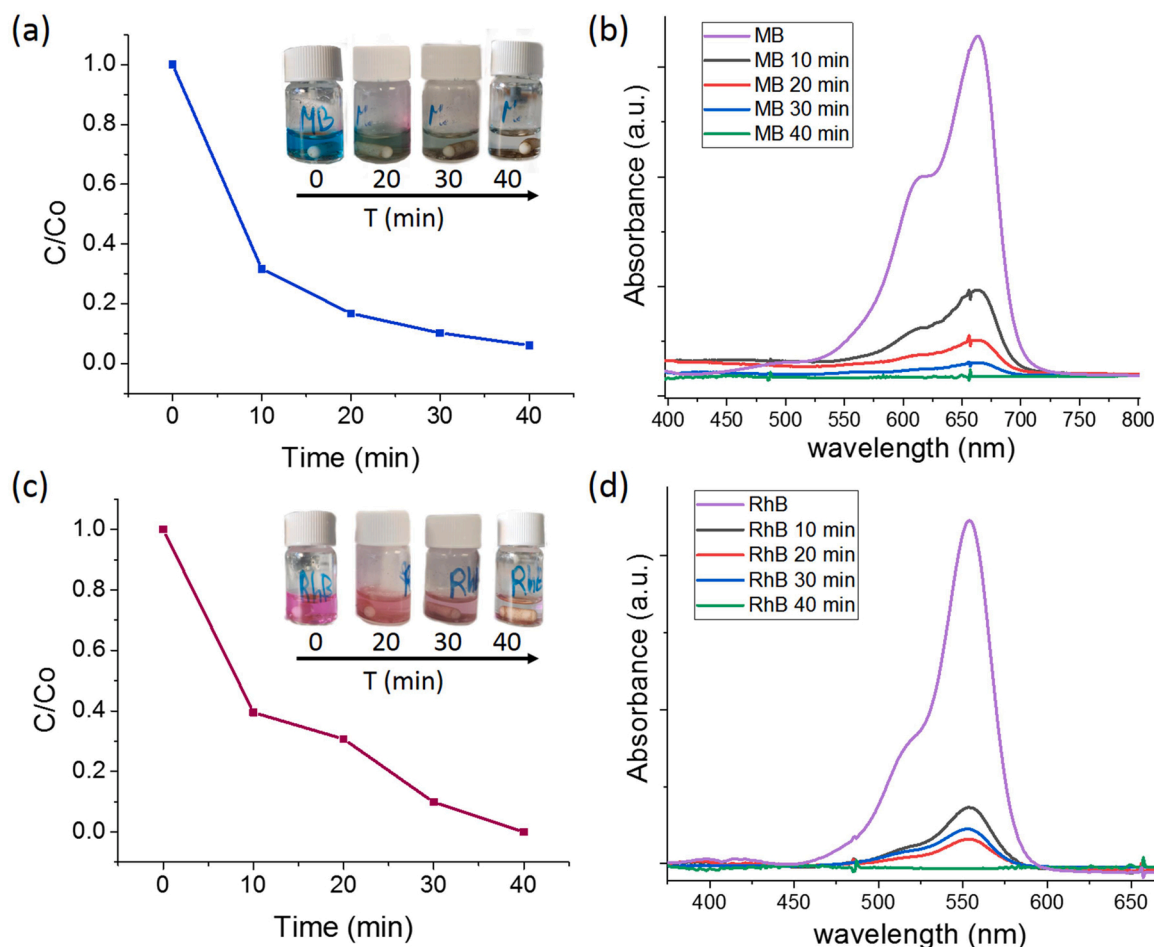


Fig. 6. Photocatalytic degradation plots of C/C_0 (concentration/initial concentration) versus t (time) of organic dye MB (a) and RhB (c) starting from a 1×10^{-5} M solution of both dyes catalyzed by CP4 after illumination with a white light photoreactor (300–600 nm). Absorbance measurements to check the degradation of MB (b) and RhB (d) dyes.

With these results, we have proceeded to study the photocatalytic capacity of **CP1** and **CP4**, against the dye degradation in water.

3.7. Photocatalytic degradation of organic dyes with CP1 and CP4

Wastewater from the textile industry contains significant concentrations of organic matter that contribute to the toxicity of the effluents. It is well known that the stability and high degree of aromaticity in azo-dyes prevent the mineralization of these compounds by conventional aerobic biological treatment processes. Thus, there is currently considerable interest in developing alternative techniques that can degrade organic pollutants and be more cost-effective and environmentally benign.[23,24] Among others, catalysis is a powerful tool for such purposes and different kinds of processes have been developed, mainly for the oxidation of organic pollutants. For this reason and given that the photocatalytic activity of the Cu(I)-halogen coordination polymers has almost not been studied, we have decided to explore their activity in the degradation of persistent dyes such as methylene Blue (MB) or Rhodamine B (RhB) present in water [13,25–28]. For this, five standard solutions of organic dyes with concentrations from 0 to 10^{-5} M were prepared, and knowing the absorbance of each of them with UV equipment, their corresponding calibration line was obtained (with R^2 0.999) that will be used later (Figs. S23 and S24) to quantify the absorbance of dye that degrades as a function of time (Fig. 6b and d). The photocatalytic behavior due to solar light was studied using a photoreactor. For each experiment, 2 mg of **CP1** and **CP4** respectively were mixed with 2 mL of an aqueous solution (10^{-5} M) of the

corresponding dye and were excited at a wavelength of 300–600 nm. Mention that in the case of **CP1** no MB degradation has been observed over time. However, **CP4** has shown a high capacity to degrade both MB and RhB. One of the possible causes of the inactivity of **CP1** compared with **CP4** may be related to the number of active centers (metal ions) per area, since **CP1** is a one-dimensional coordination polymer, being also the most stable compound both thermodynamically and kinetically, and **CP4** is a two-dimensional compound with laminar structure. In the case of **CP4**, at the beginning ($t = 0$) the spectrum showed an intense absorption peak of MB and RhB at 660 and 550 nm respectively (Fig. 6d and d). As time progressed, the photocatalysis reaction of the organic dye led to a continuous decline of the absorption peak intensity which designated the degradation of MB and RhB. Every 10 min an aliquot of the dye is analyzed using UV-visible to total degradation up to 40 min (Fig. 6a-d). The variation in (C/C_0) with irradiation time for **CP4** with MB and RhB is shown in Fig. 6a and c. The observed linear correlation between $\ln(C/C_0)$ and t (time) (Figs. S31–S32) indicates a first-order degradation reaction. The estimated degradation rate constant (k) is found to be, 0.072 and 0.088 min⁻¹ for the photocatalysts **CP4** and MB, and RhB respectively (Figs. S30–S31). After complete degradation of the dye, the suspension is centrifuged and the **CP4** is dried. In order to verify the stability and purity of the bulk compound after the photo degradation of the dyes for further catalytic studies, SEM images of **CP4** before and after photo-degradation of MB and RhB were compared (Fig. S32) found that after degradation and agitation inside the photoreactor the compound reduces its size. Additionally, the corresponding IR spectra (Figs. S25 and S26) and powder X-ray diffractograms (Fig. S27) have

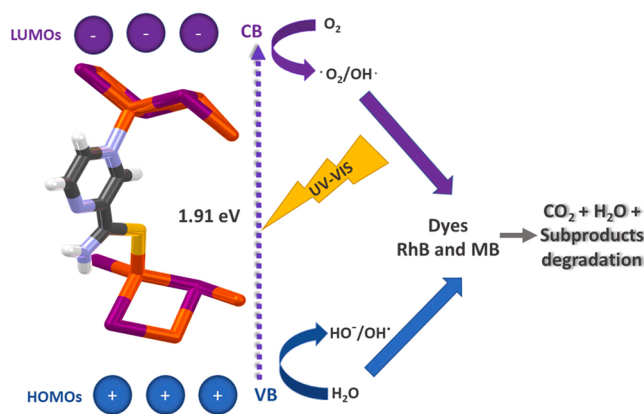


Fig. 7. Schematic representation of the photocatalytic mechanism of dyes degradation by CP4.

been performed verifying that there have been no changes in its initial structure [24].

It is noteworthy that the same CP4 sample can be used to degrade the MB and RhB dye in up to 2 cycles, although the time to achieve complete degradation increases in each cycle, with radiation exposure of 90 min being necessary for the second cycle. (Figs. S28-S29).

The mechanism of the degradation of organic dyes has been well documented. In general, under the UV-visible irradiation, electrons can be excited from the valence band (VB), transmitted to the conduction band (CB), and concurrently, positively charged holes are produced in the VB. After migrating to the surface of the catalyst, the electrons (e^-) and holes (h^+) can produce radical species (such as superoxide radicals and hydroxyl radicals), which are responsible for the degradation of dyes (Fig. 7). The anticipated mechanism for the above photodegradation should be the $^{\bullet}\text{OH}$ radical mediated route [29]. The highly active $^{\bullet}\text{OH}$ radical consequently degrades the dyes molecules upon oxidation.

4. Conclusions

This work shows the great versatility that coordination polymers have starting from the same building blocks through small modifications in the synthetic conditions. It also shows the flexibility of the CuI chains that allow obtaining polymorphs through changes in the reaction temperature. The stability and insolubility of these compounds together with their possible semiconductor character (with band gap around 2 eV) allow their use as a photocatalyst for persistent organic dyes and open the door to optimizing its photocatalytic capacity in the presence of sunlight. Moreover, the activity as photocatalyst of $[\text{Cu}_2\text{I}_2(\text{Pyrtca})]_n$ compared to $[\text{CuI}(\text{Pyrtca})]_n$ with similar band gaps may be due to its two-dimensional structure with more Cu(I) centers per unit volume. It should also be mentioned that the presence of CuI acting as a catalyst both at high temperatures and pressures and at long periods of time at room temperature exposed to air, facilitates the transformation of the pyrazine 2-thiocarboxamide to a bisulfate of an imidazole derivative, which may be of interest in the organic chemistry area. Further studies on the structural regulation and structure-photocatalytic property relationship are also in progress in our group.

CRediT authorship contribution statement

Maria Murillo: Investigation, Methodology, Validation, Writing – review & editing. **Andrea García-Hernan:** Methodology, Validation, Investigation. **Jésus López:** Investigation. **Josefina Perles:** Formal analysis, Review & Editing. **Ivan Brito:** Formal analysis. **Pilar Amo-Ochoa:** Writing - original draft, Writing - Review & Editing, Conceptualization, Visualization, Supervision. Project administration. Funding

acquisition.

Declaration of Competing Interest

The authors declare the following financial interests/personal relationships which may be considered as potential competing interests: Pilar Amo Ochoa reports that part of financial support was provided by Universidad Autónoma de Madrid.

Data availability

No data was used for the research described in the article.

Acknowledgments

We are grateful to SCXRD laboratory of the Interdepartmental Research Service (SIdI) for the structural solutions and to Agatha Bastida for her help in the antibacterial assays. This work was supported by the Spanish Ministerio de Ciencia e Innovación (Agencia Estatal de Investigación) (MCIN/AEI/10.13039/501100011033; PID2019-108028GB-C22 and TED2021-131132B-C22).

This work is dedicated to David Tudela and Félix Zamora.

Appendix A. Supporting information

Supplementary data associated with this article can be found in the online version at doi:10.1016/j.cattod.2023.114072.

References

- [1] I.M.L. Rosa, M.C.S. Costa, B.S. Vitto, L. Amorim, C.C. Correa, C.B. Pinheiro, A. C. Doriguetto, Influence of synthetic methods in the structure and dimensionality of coordination polymers, *Cryst. Growth Des.* 16 (2016) 1606–1616.
- [2] J. Conesa-Egea, F. Zamora, P. Amo-Ochoa, Perspectives of the smart Cu-Iodine coordination polymers: a portage to the world of new nanomaterials and composites, *Coord. Chem. Rev.* 381 (2019) 65–78.
- [3] K. Hassanein, J. Conesa-Egea, S. Delgado, O. Castillo, S. Benmansour, J.I. Martinez, G. Abellan, C.J. Gomez-Garcia, F. Zamora, P. Arno-Ochoa, Electrical conductivity and strong luminescence in copper iodide double chains with isonicotinato derivatives, *Chem. Eur. J.* 21 (2015) 17282–17292.
- [4] J. Conesa-Egea, J. Gallardo-Martinez, S. Delgado, J.I. Martinez, J. Gonzalez-Platas, V. Fernandez-Moreira, U.R. Rodriguez-Mendoza, P. Ocon, F. Zamora, P. Amo-Ochoa, Multistimuli response micro- and nanolayers of a coordination polymer based on Cu2I2 chains linked by 2-aminopyrazine, *Small* 13 (2017).
- [5] H. Wise, B.J. Wood, Defect structure of cuprous iodide and its catalytic properties, *J. Phys. Chem.* 71 (1967) 4517–4522.
- [6] C. Li, X. Liu, Y. Zhang, Y. Chen, T. Du, H. Jiang, X. Wang, A novel nonenzymatic biosensor for evaluation of oxidative stress based on nanocomposites of graphene blended with CuI, *Anal. Chim. Acta* 933 (2016) 66–74.
- [7] C.-H. Chang, M. Madasu, M.-H. Wu, P.-L. Hsieh, M.H. Huang, Formation of size-tunable CuI tetrahedra showing small band gap variation and high catalytic performance towards click reactions, *J. Coll. Inter. Sci.* 591 (2021) 1–8.
- [8] A. Chylewska, A. Sikorski, M. Ogryzek, M. Makowski, Attractive S \cdots π and π - π interactions in the pyrazine-2-thiocarboxamide structure: experimental and computational studies in the context of crystal engineering and microbiological properties, *J. Mol. Struct.* 1105 (2016) 96–104.
- [9] S. Ramotowska, J. Brzeski, P. Sumczynski, M. Makowski, A. Chylewska, Physicochemical and electrochemical characteristics of pyrazine-2-thiocarboxamide and its interaction ability against biomolecules, *Electrochim. Acta* 394 (2021), 139150.
- [10] M. Ogryzek, A. Chylewska, A. Króllicka, R. Banasiuk, K. Turecka, D. Lesiak, D. Nidzworski, M. Makowski, Coordination chemistry of pyrazine derivatives analogues of PZA: design, synthesis, characterization and biological activity, *RSC Adv.* 6 (2016) 52009–52025.
- [11] M. Biedulska, A. Chylewska, D. Nidzworski, Comparative solution equilibria studies of complex formation between Ir(III) ion and antituberculosis drug analogues: spectroscopic, potentiometric and conductometric approach, *J. Mol. Liq.* 296 (2019), 111887.
- [12] Y.-L. Hou, R.W.-Y. Sun, X.-P. Zhou, J.-H. Wang, D. Li, A copper(i)/copper(ii)-salen coordination polymer as a bimetallic catalyst for three-component Strecker reactions and degradation of organic dyes, *Chem. Commun.* 50 (2014) 2295–2297.
- [13] T. Wen, D.-X. Zhang, J. Zhang, Two-dimensional copper(I) coordination polymer materials as photocatalysts for the degradation of organic dyes, *Inorg. Chem.* 52 (2013) 12–14.
- [14] X. Dong, Y. Li, D. Li, D. Liao, T. Qin, O. Prakash, A. Kumar, J. Liu, A new 3D 8-connected Cd(II) MOF as a potent photocatalyst for oxytetracycline antibiotic degradation, *Crystengcomm* 24 (2022) 6933–6943.

- [15] T. Miyata, T. Namera, Y. Liu, A. Kawamura, T. Yamaoka, Photoresponsive behaviour of zwitterionic polymer particles with photodimerizable groups on their surfaces, *J. Mater. Chem. B* 10 (2022) 2637–2648.
- [16] M. Akbar Ali, S.E. Livingstone, Metal complexes of sulphur-nitrogen chelating agents, *Coord. Chem. Rev.* 13 (1974) 101–132.
- [17] E.S. Raper, Complexes of heterocyclic thionates. Part 1. Complexes of monodentate and chelating ligands, *Coord. Chem. Rev.* 153 (1996) 199–255.
- [18] A.W. Addison, T.N. Rao, J. Reedijk, J. van Rijn, G.C. Verschoor, Synthesis, structure, and spectroscopic properties of copper(II) compounds containing nitrogen-sulphur donor ligands; the crystal and molecular structure of aqua[1,7-bis(N-methylbenzimidazol-2'-yl)-2,6-dithiaheptane]copper(II) perchlorate, *J. Chem. Soc., Dalton Trans.* (1984) 1349–1356.
- [19] E. Bouwman, W.L. Driessen, J. Reedijk, Model systems for type I copper proteins: structures of copper coordination compounds with thioether and azole-containing ligands, *Coord. Chem. Rev.* 104 (1990) 143–172.
- [20] S. Guin, S.K. Rout, A. Gogoi, S. Nandi, K.K. Ghara, B.K. Patel, Desulfurization strategy in the construction of azoles possessing additional nitrogen, oxygen or sulfur using a copper(I) catalyst, *Adv. Synth. Catal.* 354 (2012) 2757–2770.
- [21] A. Gallego, O. Castillo, C.J. Gomez-Garcia, F. Zamora, S. Delgado, Electrical conductivity and luminescence in coordination polymers based on copper(I)-halides and sulfur-pyrimidine ligands, *Inorg. Chem.* 51 (2012) 718–727.
- [22] G. Givaja, P. Amo-Ochoa, C.J. Gomez-Garcia, F. Zamora, Electrical conductive coordination polymers, *Chem. Soc. Rev.* 41 (2012) 115–147.
- [23] S.E.-dH. Etaiw, S.N. Abdou, Spectroscopic properties and the catalytic activity of new organo-lead supramolecular coordination polymer containing quinoxaline, *Spectrochim. Acta Part A: Mol. Biomol. Spect.* 135 (2015) 617–623.
- [24] S. Kulovi, S. Dalbera, S. Das, E. Zangrando, H. Puschmann, S. Dalai, New silver(I) coordination polymers with hetero donor ligands: synthesis, structure, luminescence study and photo-catalytic behavior, *Chemistryselect* 2 (2017) 9029–9036.
- [25] S.-L. Li, X.-M. Zhang, Cu₃I₇ Trimer and Cu₄I₈ tetramer based cuprous iodide polymorphs for efficient photocatalysis and luminescent sensing: unveiling possible hierarchical assembly mechanism, *Inorg. Chem.* 53 (2014) 8376–8383.
- [26] X. Zheng, Y. Chen, J. Ran, L. Li, Synthesis, crystal structure, photoluminescence and catalytic properties of a novel cuprous complex with 2,3-pyrazinedicarboxylic acid ligands, *Sci. Rep.* 10 (2020) 6273.
- [27] N. Sakamoto, Y.F. Nishimura, T. Nonaka, M. Ohashi, N. Ishida, K. Kitazumi, Y. Kato, K. Sekizawa, T. Morikawa, T. Arai, Self-assembled cuprous coordination polymer as a catalyst for CO₂ electrochemical reduction into C₂ products, *ACS Catalysis* 10 (2020) 10412–10419.
- [28] A. Ghorai, J. Mondal, G.K. Patra, Photoluminescent mixed ligand complexes of CuX (X=Cl, Br, I) with PPh₃ and a polydentate imino-pyridyl ligand – syntheses, structural variations and catalytic property, *J. Mol. Struct.* 1097 (2015) 52–60.
- [29] J.-F. Wang, S.-Y. Liu, C.-Y. Liu, Z.-G. Ren, J.-P. Lang, Silver(I) complexes with a P–N hybrid ligand and oxyanions: synthesis, structures, photocatalysis and photocurrent responses, *Dalton Trans.* 45 (2016) 9294–9306.